3rd URSI AT-AP-RASC, Gran Canaria, 29 May – 3 June 2022

Simulation of 5G MU-MIMO radiation patterns in the 3.5 GHz band in urban environments for future EMF exposure assessment

Nicolas Noé*(1) and François Gaudaire(1)
(1) CSTB, Acoustics Vibration Lighting and Electromagnetism Division, France

Abstract

In this paper we study the influence of the built environment on the shape of radiation patterns of 5G MU-MIMO beamforming antennas, using simulation, to better characterize the downlink exposure in future 5G networks. A real database of existing and future 5G sites is used as a corpus of test sites. Simulations of beamforming on these sites lead to a large set of radiation patterns, each pattern representing the time averaged behavior of an antenna. The distribution of the intrinsic parameters of these patterns (gain, apertures) are then analysed and compared to an envelop pattern of all beam directions.

1 Introduction

In previous work [4] we showed the influence of the built environment on the shape of the radiation pattern of 5G antennas doing beamforming for MU-MIMO in the 3.5 GHz band by using simulation. The locations of user equipments (UEs) in the vicinity of an antenna (in buildings and in the streets) steer beams toward preferred directions. The guidelines for EMF exposure simulation in France [1] rely on using an envelop pattern of all possible beam directions with an attenuation factor handling for usage. These guidelines are used for estimating the exposure level in the surrounding area of the antenna, and especially the maximum level. In this paper we perform simulations on a large set of realistic 5G base stations in the 3.5 GHz doing beamforming in order to be able to compare envelop or average a priori diagrams with individual ones. This approach differs with the ones in [2] (where a statistical model of overall exposure is defined) and in [3] since we focus on the radiation pattern itself and use existing real sites instead of stochastic material.

This paper is organized as follows. In section 2 we will present the numerical models used for simulation (antennas and built environment), devised from real sites. Then we will briefly present the simulation method in section 3. Finally in section 4 we will analyze results and compare simulated patterns to all-directions average pattern and conclude.

2 Numerical model

2.1 Sites

The sites to study where extracted from the French Cartoradio database, that lists all authorized radioelectric emitters in France. We filtered the database in order to only extract 5G NR beamforming antennas in the 3.5 GHz band (already in use or not), and focused on the urban area of the city of Nantes. This led to 110 sites (a site is associated to a base station of an operator) as illustrated on figure 1.

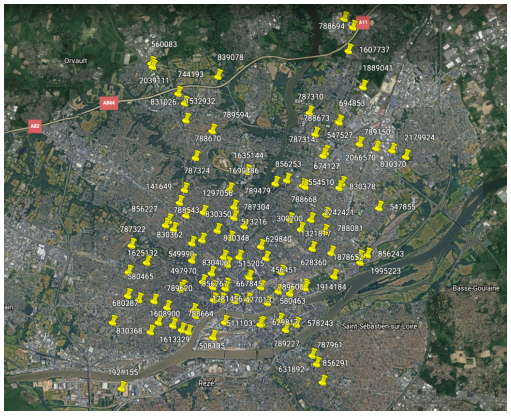

Figure 1. 5G NR sites in the 3.5 GHz deployed in the urban area of Nantes (France)

Some sites were ignored because they are either irrelevant to our study (antennas on a mast in an open environment with buildings) or were plagued with obvious errors in the available building model (missing buildings or with erroneous shape or height). The final dataset is made of 87 base stations with a total of 254 antennas (as there are most of the time three azimuths per base station).

2.2 Buildings

The buildings were extracted from the French IGN BD-TOPO database. In the considered urban area, most of the buildings are given by their ground footprint and height. As previously mentioned only sites with buildings correctly matching the real environment are kept. See figure 2 for instance.

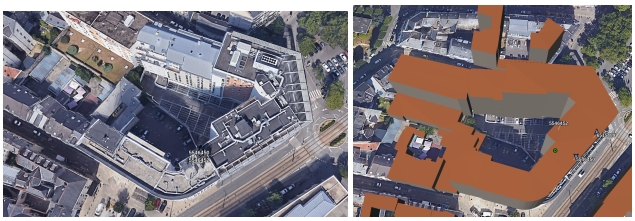

Figure 2. 3D view of an existing site (left), numerical model with buildings and fixed antenna locations (right)

2.3 Antenna

The antenna model used for the simulation mimics the existing Ericsson Air 6488 in the 3.5 GHz band. This antenna consists of 64 TRX in 4 rows and 8 columns. The numerical model uses a tuned 3GPP radiation pattern for each of the 64 subelements (as 32 pairs of two subelements). The horizontal and vertical spacing are also tuned to match with the manufacturer radiation pattern.

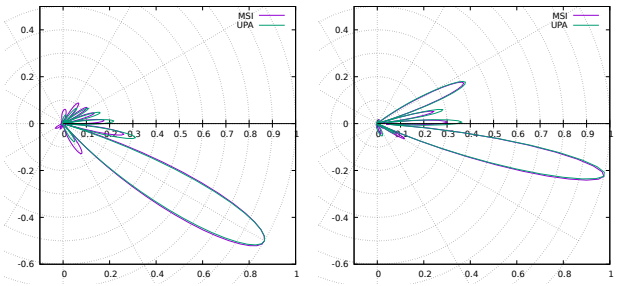

Figure 3. Far field horizontal (left) and vertical linear radiation pattern of Ericsson AIR 6488 antenna : manufacturer data (aquamarine) and numerical model (magenta) for a beam steered 30° horizontally and -13° vertically

Using this numerical antenna model, beamforming can be performed in any direction by controlling the weight (power and phase) of each subelement. The horizontal scan is $\pm 60°$ and the vertical scan is $\pm 20°$. The antenna is mechanically tilted downward to cover the simulation area. In far field the radiation pattern of the numerical model closely matches with the manufacturer datasheet as illustrated on figure 3.

3 Simulations

The dynamic pattern behavior is simulated as in [4]. First a large number of UEs are randomly distributed on the ground (20%) and inside the buildings (80%) in the vinicity of the base station. Next, the channel between each antenna subelement and UE is computed using ray-tracing algorithm. At last, the antenna beamforms, selecting UEs to be served, using MU-MIMO zero-forcing technique. Two scenarios are studied: one with a constant drop duration for each UE, and one with a given quantity of data to be downloaded for each UE (hence taking into account throughput). Once an UE is served, it is forgotten, so there are as many UEs as needed to have a stable time averaged antenna pattern (here 1280 UEs per antenna).

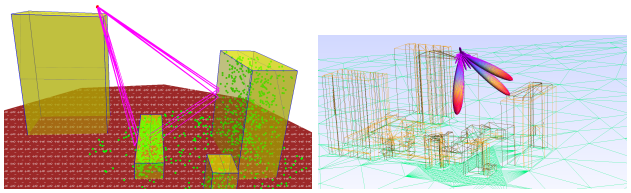

Figure 4. Simulation method: ray-tracing for channel computation (left) and beamforming (right, here serving 3 UEs simultaneously)

The simulations are carried for every site, in a 150 m circle around the base station location. An example of simulation is illustrated on figure 4.

4 Results

4.1 Radiation patterns

For each of the 254 simulated antennas, the pattern is time-dependant. This pattern is then averaged over time to get a unique and constant pattern per antenna. As previously stated, the shape of the resulting pattern is influenced by the location of the UEs, hence the buildings around the antenna. Some examples of patterns are shown on figure 5.

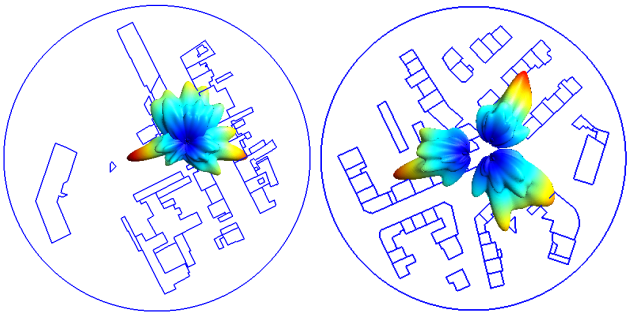

Figure 5. Examples of time-averaged patterns simulated for two different sites with three azimuths (all three antennas are colocated on the left subfigure)

4.2 Analysis

Using these 254 patterns, we extract intrinsic patterns parameters : maximum value, gain, horizontal and vertical apertures and relative azimuth (the relative azimuth is the difference between the azimuth of the antenna and the horizontal direction of the main lobe in the simulated pattern). We can then compute the probability density function (PDF) associated to these parameters, see figures 6 and 7 for the horizontal and vertical apertures and 8 for the gain. The PDFs also exhibit the value of the parameters for the *a priori* averaged radiation pattern (made by averaging the patterns in all steerable beam directions).

The gain of the average of all simulated patterns is 3.5 dB higher than the gain of the average pattern on all beam directions. That means that each of the 254 radiation patterns

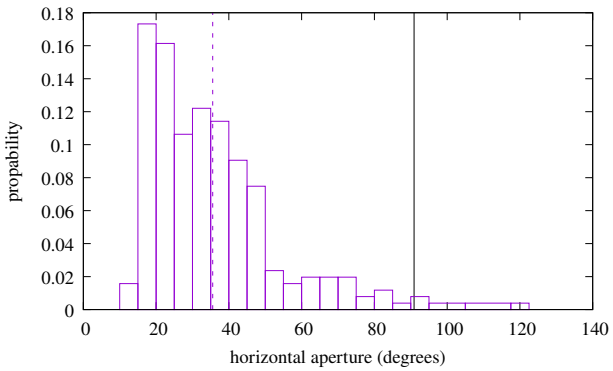

Figure 6. Distribution of the time-averaged horizontal aperture over all sites (average horizontal aperture as a dashed vertical line) and horizontal aperture of the average diagram (black vertical line)

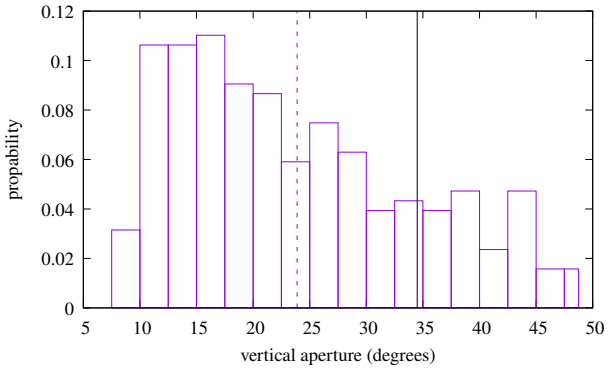

Figure 7. Distribution of the time-averaged vertical aperture over all sites (average vertical aperture as a dashed vertical line) and vertical aperture of the average diagram (black vertical line)

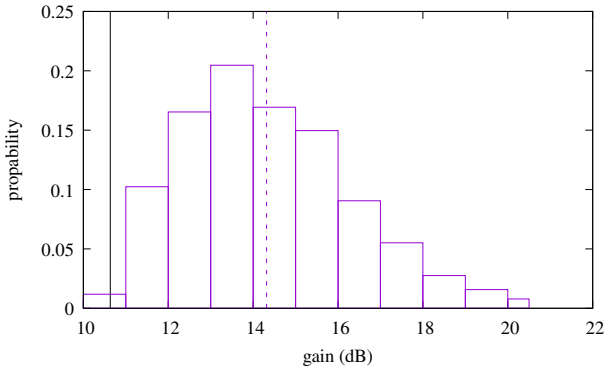

Figure 8. Distribution of the time-averaged gain over all sites (average gain as a dashed vertical line) and gain of the average diagram (black vertical line)

is slightly more directive than the average. The same behavior happens with horizontal and vertical apertures, with narrower individual main lobes. This is confirmed by the visual impact of the diagrams on figure 5. This means that the maximum exposure level (in the main lobe) might be 50% higher (in V/m) that expected with the average pattern.

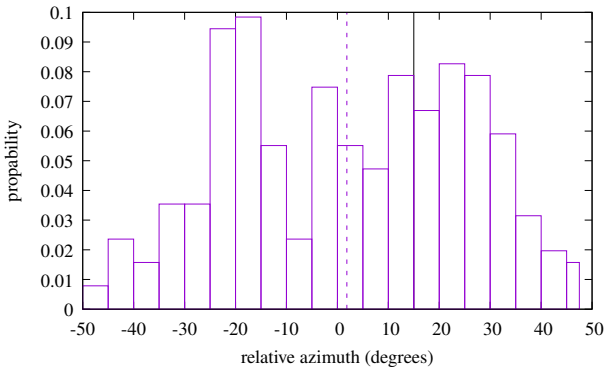

Figure 9. Distribution of the relative azimuth over all sites (average relative azimuth as a dashed vertical line)

The relative azimuth (see figure 9) also exhibits the adaptation of the antenna to its environment. The average value is almost zero but its spans a wide range of values of angles. Nevertheless this relative azimut angle is less significant than other parameters because it is a very sensitive data. In fact a change of a fraction of dB in the peak value of the pattern can drastically change the azimuth value for a non very directive pattern.

We also average all these 254 patterns in a single one (*a posteriori* average) and compare it to *a priori* pattern on figure 10. The vertical patterns are almost identical (keeping the secondary lobes) while the horizontal patterns are very close (the *a posteriori* average looking more like an envelop of all horizontal directions).

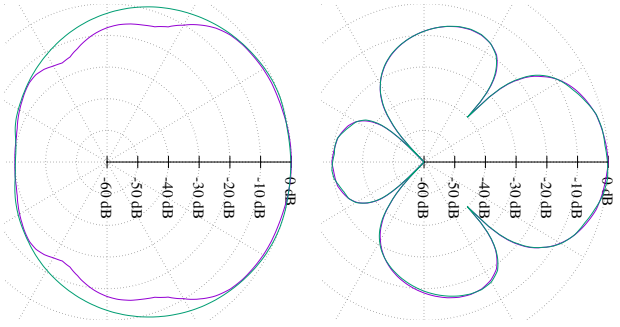

Figure 10. Comparison of the horizontal (left) and vertical (right) patterns : average simulated pattern (aquamarine curve, average of simulated patterns for all 254 antennas) and average beam pattern (magenta curve, made by averaging all possible individual beams within the scan range)

In this paper results are presented for the constant drop duration scenario ; results for the other scenario are equivalent.

5 Conclusion

In this original study we have used existing realistic 5G MU-MIMO sites, ray tracing simulations and simplified network scenarios (zero forcing) to determine 5G radiation patterns. Nevertheless the results outline that while averaged patterns are suitable for EMF exposure prediction, the variability in each particular situation must be taken into account. These results can be used to estimate the error between an envelop or average pattern and the effective pattern. It would also be possible to have more than one envelop pattern by analyzing correlation between the intrinsic parameters of the simulated patterns and geometrical parameters of the environment (building density and visibility as seen from the antenna). All these results also have to be confirmed by measurements when the simulated base stations will be fully deployed.

References

[1] ANFR, "Lignes directrices nationales sur la présentation des résultats de simulation de l'exposition aux ondes émises par les installations radioélectriques," *Tech. report, ANFR*, October 2019, `https://www.anfr.fr/fileadmin/mediatheque/documents/expace/20191001-Lignes-directrices-nationales.pdf`.

[2] M. A. Hajj, S. Wang, P. d. Doncker, C. Oestges and J. Wiart, "A Statistical Estimation of 5G Massive MIMO's Exposure using Stochastic Geometry," *2020 XXXIIIrd General Assembly and Scientific Symposium of the International Union of Radio Science*, 2020, pp. 1-3, doi: 10.23919/URSIGASS49373.2020.9232290.

[3] T. Jiang and A. K. Skrivervik, "Assessment of the Electromagnetic Field Exposure due to 5G Base Stations using a Monte-Carlo Method: Initial Results," *2021 15th European Conference on Antennas and Propagation (EuCAP)*, 2021, pp. 1-4, doi: 10.23919/EuCAP51087.2021.9411041.

[4] N. Noé and F. Gaudaire, "Numerical Modeling of the Effect of the Built Environment and Usages on Downlink EMF Exposure Induced by MU-MIMO 5G Antennas," *2021 XXXIVth General Assembly and Scientific Symposium of the International Union of Radio Science*, 2021, pp. 1-4, doi: 10.23919/URSIGASS51995.2021.9560503.